Different levels of the Tripartite motif protein, Anomalies in sensory axon patterning (Asap), regulate distinct axonal projections of *Drosophila* sensory neurons

Rei K. Morikawa[a,b], Takahiro Kanamori[a,b], Kei-ichiro Yasunaga[a,b], and Kazuo Emoto[a,b,c,1]

[a]Department of Cell Biology, Osaka Bioscience Institute, Suita, Osaka 565-0874, Japan; [b]Neural Morphogenesis Laboratory, National Institute of Genetics, Mishima, Shizuoka 411-8540, Japan; and [c]Core Research for Evolutional Science and Technology, Japan Science and Technology Agency, Chiyoda, Tokyo 102-0075, Japan

Edited by Shigetada Nakanishi, Osaka Bioscience Institute, Suita, Japan, and approved October 3, 2011 (received for review June 21, 2011)

The axonal projection pattern of sensory neurons typically is regulated by environmental signals, but how different sensory afferents can establish distinct projections in the same environment remains largely unknown. *Drosophila* class IV dendrite arborization (C4da) sensory neurons project subtype-specific axonal branches in the ventral nerve cord, and we show that the Tripartite motif protein, Anomalies in sensory axon patterning (Asap) is a critical determinant of the axonal projection patterns of different C4da neurons. Asap is highly expressed in C4da neurons with both ipsilateral and contralateral axonal projections, but the Asap level is low in neurons that have only ipsilateral projections. Mutations in *asap* cause a specific loss of contralateral projections, whereas overexpression of Asap induces ectopic contralateral projections in C4da neurons. We also show by biochemical and genetic analysis that Asap regulates Netrin signaling, at least in part by linking the Netrin receptor Frazzled to the downstream effector Pico. In the absence of Asap, the sensory afferent connectivity within the ventral nerve cord is disrupted, resulting in specific larval behavioral deficits. These results indicate that different levels of Asap determine distinct patterns of axonal projections of C4da neurons by modulating Netrin signaling and that the Asap-mediated axonal projection is critical for assembly of a functional sensory circuit.

Information from the external environment is transmitted to the CNS by sensory neurons, and the neuronal circuits that process sensory information are established in part through the projection of terminal sensory axon branches to specific target zones (1–5). In many sensory systems, the pattern of axonal projection is shaped by environmental cues that provide positional or directional signals to the developing axons (3–5). However, many sensory neurons encountering the same environment establish distinctive axonal terminal patterns, suggesting that distinct neuronal types have different capacities to respond to a given environmental cue. A well-studied intrinsic mechanism for accomplishing this differential response is to vary receptors for the environmental cues, thus allowing each neuron type to interpret the environmental information uniquely (4–6). Upon ligand binding, the receptors transduce signals to the cytoskeleton to control steering decisions (6). Therefore, another potential mechanism for regulating a neuron's response to environmental cues is to regulate intracellular signaling differentially downstream of the receptors. In theory, distinct classes of neurons could shape distinctive axonal projection patterns by differentially modulating the intracellular signaling to the cytoskeleton downstream of a common receptor. In contrast to the accumulating evidence supporting the role of guidance receptors in the axonal projection, much less is known about the role of the downstream regulators in divergent patterns of axonal projections in vivo.

The class IV dendrite arborization (C4da) sensory neurons in the *Drosophila* peripheral nervous system (PNS) provide an in vivo system for investigating the molecular mechanisms that regulate distinct sensory axon projections (7, 8). C4da neurons comprise three subtypes positioned at distinct regions in each abdominal hemisegment: ddaC, v'ada, and vdaB (Fig. 1*A*; see also Fig. S2*C*). In contrast to the similar patterns of their dendrite arbors on the epidermis (9), the three C4da subtypes exhibit distinctive branching patterns of axonal terminals in the ventral nerve cord (VNC). Upon entering the VNC, the v'ada axons extend terminal branches along the longitudinal axis and likely synapse onto neurons on the ipsilateral side, whereas the ddaC and vdaB neurons additionally develop terminal branches projecting across the midline to form synapses on the contralateral side (7). These structures suggest that the three C4da subtypes project distinctive axonal terminals in response to the same environmental cues in the VNC, but the origin of the subtype-specific differences in C4da axonal arborization remains unknown.

To explore molecular mechanisms responsible for the specific projection pattern of distinct C4da neuron axons, we performed a genetic screen for mutants specifically defective in the axonal patterning in C4da neurons and identified the protein Anomalies in sensory axon patterning (Asap) as an axon-specific determinant for the subtype-specific contralateral projections in C4da neurons. Further genetic and biochemical analyses indicate that Asap modulates Netrin signaling. Our findings suggest that Asap establishes distinct patterns of sensory axon projections by altering the susceptibility of each C4da subtype to the environmental cue Netrin in a dose-dependent manner and contributes to the assembly of the functional sensory circuits that involve perception through C4da neurons.

Results

***asap* Mutants Are Specifically Defective in Axonal Patterning of C4da Neurons.** To identify genes required for contralateral projection of C4da neurons, we carried out a genetic screen using *pickpocket-EGFP* (*ppk-EGFP*), a specific marker for C4da neurons (10). *ppk-EGFP* visualizes the axonal terminal branches of C4da neurons in the VNC as a ladder-like pattern with a longitudinal fascicle on each side and a commissural fascicle in every segment (Fig. 1*A*). From ~300 mutant lines carrying PiggyBac transposon (PBac) insertions on the second chromosome, we isolated one PBac insertion line that shows a marked loss of the commissural fascicles at the third-instar larval stage (1.8 ± 0.8% defective in WT, $n = 22$; 92.5 ± 2.2% in $asap^{PBac}/Df$, $n = 24$) (Fig. 1 *A* and *B*). The axonal defects already were visible in stage-17 embryos (Fig. S1 *A* and *B*), suggesting that the axonal phenotypes in *asap* mutants result from defects in the initial development of the axonal branches rather than from degeneration of normally formed axons. In contrast to the robust axonal phenotypes, no obvious defects were detectable in dendrite growth and branching in *asap*-

Author contributions: R.K.M. and K.E. designed research; R.K.M. performed research; T.K. and K.-i.Y. contributed new reagents/analytic tools; R.K.M. and K.E. analyzed data; and R.K.M. and K.E. wrote the paper.

The authors declare no conflict of interest.

This article is a PNAS Direct Submission.

[1]To whom correspondence should be addressed. E-mail: emoto@obi.or.jp.

This article contains supporting information online at www.pnas.org/lookup/suppl/doi:10.1073/pnas.1109843108/-/DCSupplemental.

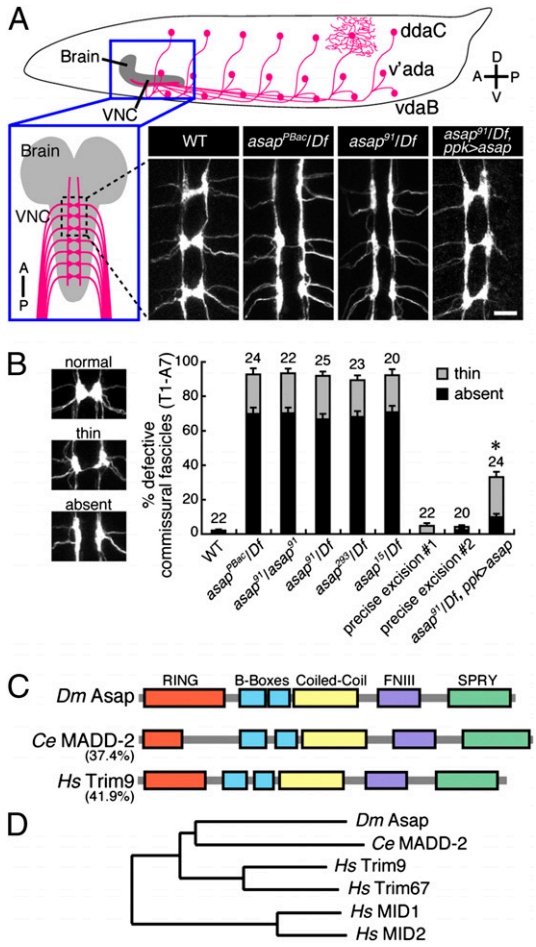

Fig. 1. *asap* mutants are defective in axonal patterning of C4da neurons. (*A*) *asap* mutants lose commissural fascicles of C4da axonal terminals. The upper diagram shows a representative lateral view of dendritic arborization and axonal projections of C4da neurons in the third-instar larva. Abdominal segments A1–A7 are shown. The CNS is indicated by blue lines. The lower diagram shows a representative ventral view of the axonal terminal projections of C4da neurons in the VNC. Photographs show live images of C4da axonal terminals of segments A1–A3 visualized by the *ppk*-EGFP reporter in WT, $asap^{PBac}$ over a deletion that uncovers *asap* ($asap^{PBac}$/*Df*), $asap^{91}$ over a deletion that uncovers *asap* ($asap^{91}$/*Df*), and $asap^{91}$/*Df* expressing Asap specifically in C4da neurons under the control of *ppkGal4* ($asap^{91}$/*Df, ppk* > *asap*). (Scale bar, 20 μm.) (*B*) Quantification of the commissural fascicle defects of C4da neurons of segments T1–A7 (T, thorax; A, abdomen) in WT and *asap* mutants. Representative images of C4da commissural fascicles categorized as normal, thin and absent are shown (*Left*). Error bars indicate SE. Numbers above the bars indicate the number of animals observed. *$P < 0.001$ compared with $asap^{91}$/*Df*, calculated for the values of absent + thin by student's *t* test. (*C*) Domain structures of Asap and its homologous proteins, MADD-2 and Trim9. MADD-2 and Trim9 show 37.4% and 41.9% amino acid homology to Asap, respectively. (*D*) A phylogenetic tree of a TRIM family subgroup containing Asap.

mutant C4da neurons (Fig. S1 *C–E*). These observations indicate that *asap* mutants are specifically defective in the axonal patterning of C4da neurons. We named this PBac mutant $asap^{PBac}$.

Inverse PCR-based mapping revealed that the PBac transposon is inserted into the first intron of CG31721 (Fig. S1*F*). To determine whether loss of CG31721 function causes the axonal phenotypes in $asap^{PBac}$, we generated null alleles ($asap^{91}$, $asap^{293}$, and $asap^{15}$) of CG31721 by imprecise excision of a P-element NP4638 inserted in the 5′ UTR of CG31721 (Fig. S1*F*). Animals homozygous for each of these alleles as well as heterozygous combinations with a chromosomal deficiency (*Df*) that uncovers CG31721 showed phenotypes in the commissural fascicles of C4da neurons identical with those observed in transheterozygous animals for $asap^{PBac}$ and the *Df* (Fig. 1 *A* and *B*). In contrast, animals homozygous for precise excisions of the P-element showed virtually no significant defects in the commissural fascicles of C4da neurons (Fig. 1*B*). Furthermore, C4da neuron-specific expression of the *asap* gene largely rescued the axonal defects in *asap*-null mutants (Fig. 1 *A* and *B*; 91.6 ± 1.8% defective in $asap^{91}$/*Df*, $n = 25$; 32.9 ± 3.0% defective in $asap^{91}$/*Df, ppk* > *asap* animals, $n = 24$), demonstrating that cell-autonomous expression of *asap* is sufficient to ensure proper axonal terminal arborization. These data demonstrate that the defects in the axonal terminal structure of C4da neuron result from loss of CG31721 function, and we thus concluded that *asap* corresponds to CG31721.

asap encodes a member of the Tripartite motif (TRIM) family of proteins, which are characterized by a tripartite motif composed of a Really Interesting New Gene (RING) domain, one or two B-Box domains, and a coiled-coil region (11). Asap additionally contains a fibronectin type III (FNIII) domain and a spla kinase and ryanodine receptor (SPRY) domain in the C terminus (Fig. 1*C*). Of more than 50 TRIM proteins found in mammals, Asap shows the highest homology to a subgroup that contains Trim9, Trim67, midline 1 (MID1; Trim18), and midline 2 (MID2; Trim1) (Fig. 1 *C* and *D*). *Drosophila* and *Caenorhabditis elegans* each have a single gene, *asap* and *muscle arm development defective (madd)-2* respectively, that belongs to this subgroup (Fig. 1 *C* and *D*).

Single-Cell Analysis of *asap* Function in C4da Neurons. To characterize the axonal phenotypes of *asap* mutants further, with higher resolution, we examined the axonal terminal morphology of individual C4da neurons using the Flp-out mosaic system. Briefly, we used the C4da-specific *ppkGal4* to express the *UAS-FRT-CD2-FRT-CD8-GFP* cassette and generated flippase (FLP)-mediated GFP-labeled single-neuron clones with all other C4da neurons labeled with CD2 (7). As previously reported (7), in WT animals, ddaC and vdaB neurons projected both ipsilateral and contralateral branches in the innervating segments, but the terminal branches of v'ada axons had only ipsilateral projections (Fig. 2*A*). We found that ddaC and vdaB axons occasionally showed additional contralateral projections in either or both of the anterior and posterior neighboring segments (for anterior and posterior neighboring segments, ddaC 11% and 11%, respectively, $n = 29$; vdaB, 50% and 5%, respectively, $n = 21$) (Fig. 2*A*). In contrast, almost no obvious contralateral projection was found in *asap* mutants, although the frequency of longitudinal branches was comparable to that in WT (Fig. 2*A*). These data indicate that the defects in the commissural fascicles in *asap* mutants result from the specific loss of the contralateral projections in ddaC and vdaB axons.

3D image reconstruction of axonal terminals revealed that the commissural branches appeared to be composed of highly branched and tangled processes and were morphologically distinct from the longitudinal fibers that appeared straight and unbranched (Fig. S1 *G* and *H*). The terminal processes were oriented almost exclusively to the medial side in all subtypes (Fig. 2 *B* and *C* and Fig. S1 *G* and *H*). Interestingly, although similar highly branched processes were visible in all subtypes of *asap* C4da neurons, the processes were oriented rather symmetrically in both medial and lateral directions (Fig. 2 *B* and *C* and Fig. S1 *G* and *H*), indicating that Asap is required for the medial orientation of terminal processes but is dispensable for branching. Taken together, our data demonstrate that Asap is required for the contralateral projections in ddaC and vdaB neurons and for the asymmetric orientation of the axonal terminal processes in all subtypes of C4da neurons.

Asap Is Differentially Expressed in C4da Neurons. Given that *asap* is likely to function in all three subtypes of C4da neurons, we verified endogenous Asap expression in C4da neurons by immunostaining. Anti-Asap immunoreactivity was found predominantly in the nervous system (Fig. 3*A* and Fig. S2). No significant immunoreactivity was detectable in *asap*-null mutant embryos (Fig. S2*B*), confirming that the Asap antibody specifically recognizes endogenous Asap protein. Asap expression was detect-

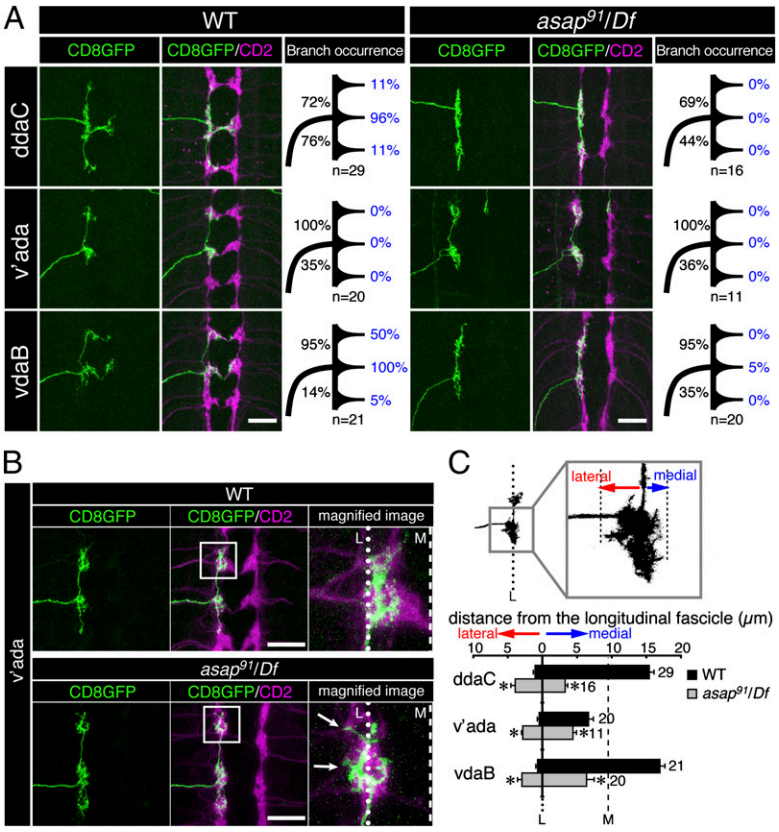

Fig. 2. Single-cell analysis of *asap* C4da neurons. (*A*) Flp-out analysis of C4da axonal projection in the VNC. Single C4da axonal terminals were labeled with CD8GFP and other C4da neurons were labeled with CD2 in WT and *asap*-null mutant (*asap*^{91}/*Df*) third-instar larvae. Representative images of ddaC, v'ada, and vdaB axonal terminals are shown. The diagram at the right of each image shows the occurrence of longitudinal branches and contralateral projections in the innervating and neighboring segments. (Scale bars, 20 μm.) (*B*) Axon terminal processes of single-labeled v'ada neurons in WT and *asap*-null mutant (*asap*^{91}/*Df*) animals. Boxed regions are enlarged in the right panels. White arrows indicate axonal processes ectopically extending laterally from the longitudinals. L (dotted line), longitudinals; M (dashed line), midline. (Scale bars, 20 μm.) See Fig. S1 *G* and *H* for images of terminal processes in WT and *asap*-mutant ddaC neurons. (*C*) Diagram and quantification of the lateral–medial orientation of the axon terminal processes. Distances between the longitudinal fiber and the lateral tip (red arrow) or the medial tip (blue arrow) of the terminal processes of single axons were measured. Terminal processes formed in the innervating segments were analyzed. L (dotted line), longitudinal position shown as reference; M (dashed line), average position of midline. Numbers to the right of the bars indicate the number of neurons observed. Error bars indicate SE. *$P < 0.005$ (student's *t* test).

able in PNS neurons first at embryonic stages 13–14, the periods in which PNS neurons start to extend axons toward the VNC, and persisted throughout the embryonic stages. In the PNS, Asap was detected in a subset of neurons including all C4da neurons labeled with *knotGal4*, a marker for C4da neurons (12, 13) (Fig. 3*A*, arrows, and Fig. S2*C*). Notably, the expression level of Asap appeared significantly stronger in ddaC and vdaB neurons than in v'ada neurons (5.5- and 3.4-fold, respectively, as compared with v'ada) (Fig. 3 and Fig. S2*C*). Thus, C4da neurons with high Asap levels elaborate contralateral projections, but those with relatively lower levels exhibit no obvious contralateral projections. These data suggest that the level of Asap expressed by different C4da neurons might determine the axonal projection patterns.

Asap Overexpression in v'ada Neurons Induces Ectopic Contralateral Projections. Based on the loss-of-function phenotypes (Figs. 1 and 2) and the patterns of Asap expression in C4da neurons (Fig. 3), we hypothesized that subtype-specific axonal patterning might be regulated by different levels of Asap. Specifically, low levels of Asap may be sufficient for asymmetric orientation of terminal processes, whereas high levels might lead to further contralateral projections. We tested this possibility by overexpressing Asap in v'ada neurons that normally show low Asap levels and whose axons have no contralateral projections. Using the mosaic analysis with a repressible cell markers (MARCM) system (14), we found that overexpression of Asap specifically in v'ada neurons caused ectopic formation of contralateral projections: 26.9% of cells ($n = 26$) showed more than one ectopic commissural branch (Fig. 4 *A* and *B*). Furthermore, doubling the copy of the Asap transgene resulted in an even larger number of commissural branches: 43.5% of v'ada expressing two copies of *asap* showed more than one ectopic commissural branch ($n = 23$) (Fig. 4*B*). In contrast to the robust phenotypes in axonal patterning, Asap overexpression produced no obvious defects in dendrite morphogenesis in v'ada neurons (Fig. S3), reinforcing the notion that Asap function likely is restricted to axonal patterning in C4da neurons. These results further demonstrate that Asap regulates distinct aspects of axonal patterning in a dose-dependent manner (Fig. 4*C*).

Asap Functions in the Netrin Pathway to Control Axonal Projections. To elucidate the molecular mechanisms of the Asap functions in the axonal projection of C4da neurons, we searched for mutations that cause a phenotype similar to that of *asap* mutants and found that mutants for a midline attractant, Netrin (Net), and its receptor, Frazzled (Fra), showed a virtually complete loss of commissural fascicles of C4da neurons (Fig. 5 *A* and *B*). Furthermore, the terminal processes of C4da axons in *fra* mutants appeared to lose the asymmetric orientation toward the midline (Fig. S4). In the *Drosophila* VNC, Netrin is secreted by midline glia and neurons and attracts commissural axons through Fra (15, 16). C4da neuron-specific expression of *fra* significantly rescued the axonal defects in *fra* mutants (Fig. 5 *A* and *B*), suggesting that Netrin signaling functions in a cell-autonomous manner to control the contralateral projection of C4da neurons.

To assess whether Asap functions in the Netrin pathway to control the axonal projections of C4da neurons, we overexpressed *asap* in a *fra*-mutant background. Although overexpression of *asap* in v'ada neurons caused ectopic contralateral projections in the WT background (Fig. 4 *A* and *B*), the ectopic contralateral projection phenotype was suppressed completely in a *fra*-mutant background (Fig. 5 *C* and *D*), indicating that Asap and Fra function in the same pathway to regulate C4da axonal projections.

To understand further the role of Asap in the Netrin pathway, we first examined the expression and localization of Fra in *asap* C4da neurons and found that neither the expression level nor the localization of Fra was affected significantly in *asap* C4da neurons (Fig. S5). Thus, we next examined whether Asap could associate physically with Netrin-signaling components. Using coimmunoprecipitation in S2 cells and yeast two-hybrid analysis, we found that Asap directly interacted with Fra through the SPRY domain and an actin-remodeling protein, Pico (17) through the FNIII domain (Fig. 5*E* and Fig. S6 *A*–*D*). Consis-

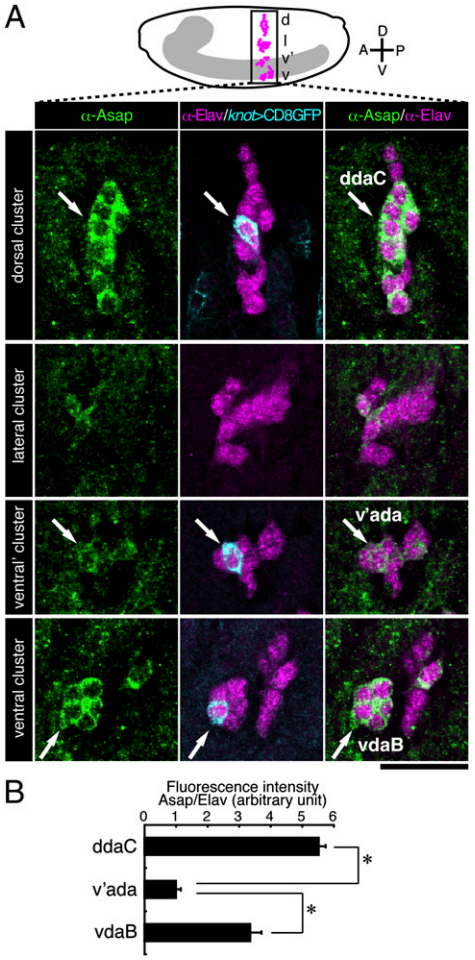

Fig. 3. Asap is expressed differentially in C4da neuron subtypes. (*A*) (*Upper*) Lateral view of a late-stage embryo with clusters of peripheral sensory neurons in a single segment. Gray region indicates the CNS, including the brain and the VNC. (Fig. S2*C* shows detailed distributions of cell bodies of sensory neurons.) d, dorsal cluster; l, lateral cluster; v', ventral' cluster; v, ventral cluster. (*Lower*) Immunostaining of peripheral sensory neurons of a stage-15 embryo. Endogenous Asap was costained with a pan-neuronal marker anti-Elav and anti-GFP that recognizes CD8GFP expressed by *knot-Gal4*, a C4da neuron-specific driver in the PNS. Arrows indicate cell bodies of C4da neurons in each PNS cluster. (Scale bar, 20 μm.) (Fig. S2 *A* and *B* shows staining patterns of the VNC and validation of the antibody.) (*B*) Relative expression levels of Asap in C4da neurons. Fluorescence intensity of the Asap signal was normalized with intensities of Elav. The normalized values are shown as arbitrary units. Error bars indicate SE. $*P < 0.001$ (student's *t* test).

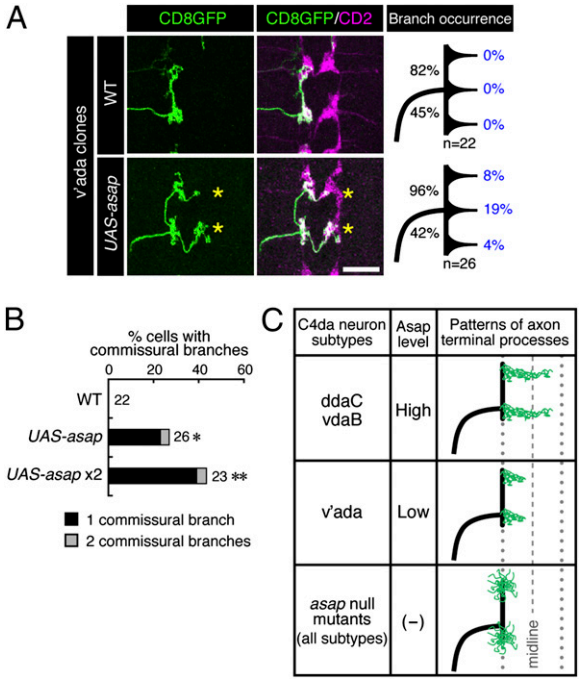

Fig. 4. Asap overexpression in v'ada neurons induces ectopic contralateral projections. (*A*) Axonal projections of WT and Asap-overexpressing (*UAS-asap*) v'ada MARCM clones in the VNC. Axonal terminals of MARCM clones were labeled with GFP (green), and all C4da neurons were labeled simultaneously with CD2 (magenta). Asterisks show ectopic contralateral projections induced by Asap overexpression. Diagrams on the right show the frequency of longitudinal and contralateral projections in MARCM clones. (Scale bar, 20 μm.) (*B*) Percentage of C4da neurons that exhibited commissural branches in WT and Asap-overexpressing v'ada MARCM clones (*UAS-asap* and *UAS-asap* x2, expressing one or two copies of *asap* transgenes respectively). $*P < 0.01$; $**P < 0.001$ (χ^2 test, compared with WT). (*C*) Summary of Asap levels and axonal projection patterns of C4da neurons. The axonal terminal processes are depicted in green. Dotted and dashed lines indicate positions of longitudinals and midline, respectively.

tently, Asap was colocalized with Fra and Pico in the terminal processes of C4da neurons (Fig. S7). In addition, Trim9, the closest human homolog of Asap, can bind directly to the Fra homologs deleted in colorectal cancer (DCC)/Neogenin (18, 19) and the Pico homolog rapid impact assessment matrix (RIAM) (20) (Fig. S6*G*), suggesting an evolutionarily conserved role of Asap/Trim9 in linking the Netrin receptors to the downstream effectors.

To examine further whether these interactions are important for the function of Asap in vivo, we performed rescue assays in which Asap proteins lacking different motifs were expressed in *asap*-mutant C4da neurons. Deletion of either the FNIII domain or the SPRY domain abrogated the ability to rescue the axonal projection defects of *asap* C4da neurons (Fig. S6 *E* and *F*), supporting the significance of the Asap–Pico and the Asap–Fra interactions for the axonal projection in C4da neurons. In addition, we found that the coiled-coil domain was required to rescue the axonal patterning defects of *asap* C4da neurons (Fig. S6 *E* and *F*). Because the coiled-coil domain likely mediates homodimerization in TRIM family proteins (21), Asap presumably functions as a homodimer in C4da neurons. In contrast, Asap proteins lacking the RING domain or the B-Box domains maintained the ability to rescue the *asap*-mutant phenotypes in C4da axons (Fig. S6 *E* and *F*), suggesting that the RING domain and the B-Box domains are dispensable for the function of Asap in C4da axonal patterning. These data indicate that interactions of Asap with Fra and Pico are essential for proper axonal projection patterns in C4da neurons and suggest a potential role of Asap in linking Fra to the downstream effector Pico in response to Netrin (Fig. 5*F*).

Asap-Mediated Axonal Projections Are Indispensable for the Function of C4da Neurons. The axonal terminals of C4da sensory neurons likely form synaptic connections with neurons in the VNC (7, 8). To examine the synaptic connectivity patterns of C4da neurons, we visualized presynaptic terminals of C4da axons by expressing synaptotagmin-GFP (Syt-GFP) in C4da neurons. We found that synaptic connections were formed on both ipsilateral and contralateral sides of the commissural branches in WT ddaC axons (Fig. S8*A*). In contrast, synaptic connections on the ipsilateral side, but not on the contralateral side, were formed in *asap* ddaC axons (Fig. S8*B*).

To test whether synaptic transmission through the Asap-mediated neuronal connections are indispensable for the function of C4da neurons, we next examined locomotion behaviors of third-instar larvae. Previous studies indicate that sensory inputs from C4da neurons modulate rhythmic locomotion behavior in

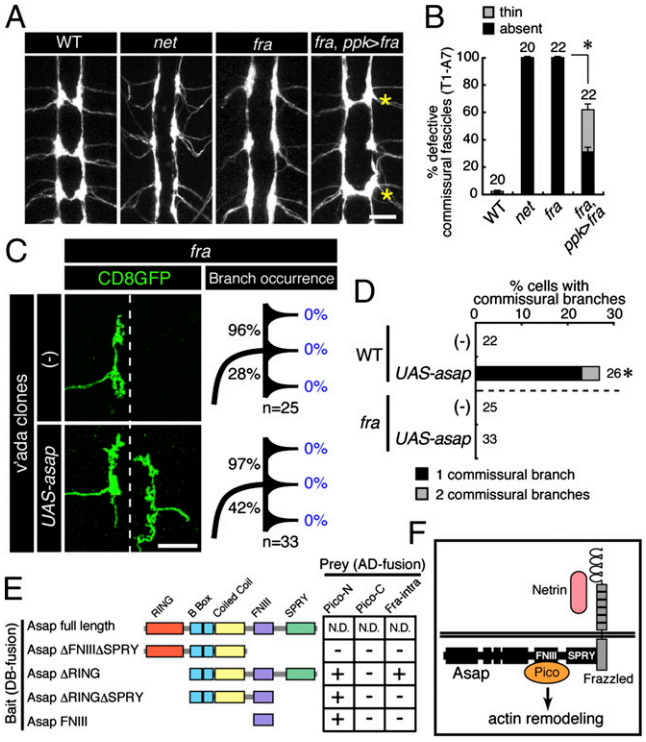

Fig. 5. Asap functions in the Netrin pathway in C4da neurons to control axonal patterning in C4da neurons. (*A*) *netrin* and *frazzled* mutants lack commissural fascicles of C4da neurons. Live images of commissural fascicles of abdominal segments A1–A3 visualized by *ppkGal4, UAS-CD8GFP* in WT, *netrin* mutants (*net*), and *frazzled* mutants (*fra*) are shown. Asterisks indicate rescued commissural fascicles. (Scale bar, 20 μm.) (*B*) Quantification of the commissural fascicle defects of C4da neurons of segments T1–A7 (T, thorax; A, abdomen) in *netrin* and *frazzled* mutants. Error bars indicate SE. $*P < 0.001$ (calculated for the values of absent + thin by student's *t* test) (*C*) Asap promotes contralateral projections through Netrin signaling in C4da neurons. Asap was overexpressed in *fra*-mutant v'ada MARCM clones (*fra, UAS-asap*). MARCM clones of indicated genotypes were labeled with CD8GFP. Diagrams on the right show the frequency of longitudinal and commissural branches. (Scale bar, 20 μm.) (*D*) Percentage of C4da neurons exhibiting commissural branches in the v'ada MARCM clones shown in *C*. Numbers to the right of the bars indicate the number of clones observed. $*P < 0.01$ [χ^2 test, compared with WT (–)]. (*E*) Summary of yeast two-hybrid analysis of interactions of Asap with Pico and Fra. N.D., not determined. Data are provided in Fig. S6C. (*F*) Summary of the role for Asap in Netrin signaling to control axonal projection in C4da neurons. In *Drosophila* VNC, Netrin is secreted by midline glia and neurons and elicits midline attraction of axons through Fra. Asap links Fra to the downstream effector Pico through the SPRY and FNIII domains, respectively, in turn inducing actin remodeling in the vicinity of Fra to promote contralateral projections and/or asymmetric orientation of the terminal processes.

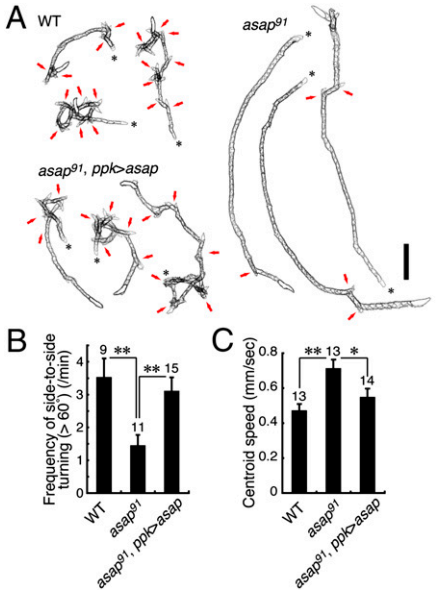

Fig. 6. *asap*-mutant larvae show less frequent turning behavior. (*A*) Contour trails of larval locomotion for 2 min. Representative trails for each genotype are shown with a starting contour indicated by an asterisk. Red arrows indicate trails of side-to-side turning behaviors. (Scale bar, 1 cm.) (*B*) Quantification of the frequency of side-to-side turning behaviors (>60°). Error bars indicate SE. Numbers above the bars indicate number of animals observed. $**P < 0.01$ (student's *t* test). (*C*) Quantification of the moving speed of larval centroids. Error bars indicate SE. Numbers above the bars indicate number of animals observed. $*P < 0.05$; $**P < 0.01$ (student's *t* test).

third-instar larvae (22–24). When placed on an aluminum block in the absence of food, WT third-instar larvae displayed a characteristic pattern of wandering behavior in which short bursts of forward movement were separated by repeated side-to-side head turnings (Fig. 6*A*). In contrast, *asap* mutants crawled with significantly fewer head-turning behaviors (Fig. 6*A* and *B*). In addition, a concomitant increase in crawling speed was observed in *asap* mutants, presumably as the result of the reduced number of turning behaviors (Fig. 6*C*). These phenotypes are similar to observations in third-instar larvae in which mechanical perception through C4da neurons has been blocked (24). Locomotion phenotypes in *asap*-mutant larvae were restored substantially by C4da neuron-specific expression of *asap* (*asap*^{91}, *ppk* > *asap* in Fig. 6), indicating that Asap expression in C4da neurons is sufficient for proper larval locomotion. Thus it is likely that the Asap-mediated contralateral connectivity in the VNC is functionally important for C4da neurons to convey sensory information properly to the VNC.

Discussion

Through a forward genetic screen, we identified a TRIM family protein, Asap, as the critical determinant of the projection pattern of axonal terminals in C4da sensory neurons. *Asap*-mutant C4da axons failed to form commissural fascicles because of the specific loss of the contralateral projections in ddaC and vdaB axons (Figs. 1 and 2), and these defects could be ameliorated substantially by expression of *asap* in mutant C4da neurons (Fig. 1), indicating that Asap functions in a cell-autonomous manner to regulate the contralateral axonal projection. We also found that axon terminal processes in v'ada neurons, as well as in ddaC and vdaB, were oriented preferentially to the midline and that this biased orientation disappeared in *asap* mutants (Fig. 2). These data indicate that Asap is required for asymmetric orientation of the axonal terminal processes in all C4da neurons as well as for contralateral projections in ddaC and vdaB axons. Given the expression patterns of Asap in C4da neurons (Fig. 3), we propose that high Asap levels promote contralateral projections and that low levels are sufficient for asymmetric orientation of the terminal processes toward the midline. In support of this model, overexpression of Asap in v'ada neurons, which express low levels of Asap, induced ectopic contralateral projections (Fig. 4).

How could Asap control axonal patterns in C4da neurons in a dose-dependent manner? Given that Asap functions through the Netrin signaling pathway, one possibility is that Asap may modulate axonal responses to the midline attractant Netrin differentially, according to its level. More specifically, Asap levels in ddaC and vdaB neurons might be high enough to respond fully to the Netrin attraction signal to form contralateral projections, whereas low Asap levels in v'ada neurons might be insufficient to induce contralateral projections but could orient them toward the midline (Fig. 4*C*). Netrin signaling has been reported to regulate diverse aspects of neuronal development, such as migration, axonal initiation, outgrowth, guidance, and synapto-

genesis (6, 25–27). For instance, in *C. elegans*, glia-derived Netrin signal facilitates axonal extension in the RIA interneuron, whereas the same Netrin signal promotes specification of presynaptic terminals but not axonal extension in the neighboring AIY interneuron (27). However, it has been unclear how the same receptor and ligand elicit diverse cellular responses in distinct neurons. Our findings suggest that Asap can modulate Netrin signaling to generate diverse neurite behaviors and thus raise the possibility that different levels of Asap in neurons may contribute to distinctive cellular responses to the same guidance cue, Netrin. Interestingly, although our immunolabeling revealed that Asap is expressed at different levels in different subsets of PNS neurons (Fig. 3*A* and Fig. S2*C*), we found that most PNS neurons appear to express similar levels of Fra receptor (Fig. S5*A*). Given that different classes of PNS neurons likely elaborate axonal arbors with distinctive projection patterns in the same VNC environment (7, 8, 28), it is conceivable that Asap levels account for the differences in response to the Netrin signal in the PNS neurons.

The mechanism that regulates Asap levels in C4da neurons currently is unknown. Previous studies have shown that specification of each sensory neuron is regulated in part by the combinatorial actions of transcription factors (12, 13, 29, 30). We have found several consensus sequences potentially recognized by specific transcription factors in the 5′ UTR and the first intron of *asap* gene. Thus, it will be of interest to determine whether these transcription factors may control Asap levels as well as axonal projection patterns in individual C4da neurons.

TRIM family proteins are characterized by the conserved Tripartite domains, including the RING domain, and several TRIM proteins likely act as E3 ligases through the RING domain to target substrates for destruction via the ubiquitin-proteasome system (31). Indeed, recent studies demonstrated that MADD-2, the nematode homolog of Asap, requires the RING domain for its roles in muscle arm extension and ventral guidance of HSN axons, implying that MADD-2 functions as an ubiquitin ligase in this context (32–34). By contrast, our genetic rescue experiments in C4da neurons revealed that the RING domain is dispensable and that instead the FNIII domain is essential for the Asap function in axonal projection, presumably by promoting Asap–Pico interaction (Fig. 5 *E* and *F* and Fig. S6 *A*–*F*). These results suggest that Asap/MADD-2 may have distinct functions in different cellular contexts.

Our behavioral analysis suggests that the Asap-mediated axonal projections in the VNC are essential for functional circuits to process properly the sensory information that is received by C4da neurons (Fig. 6). Trim9, a mammalian homolog of Asap, is expressed specifically in the nervous system (35). Given that Trim9 and Asap likely link the Netrin receptors to the downstream effectors (Fig. S6*G*), Asap/Trim9 might play a conserved role in formation of functional neuronal circuits by modulating Netrin signaling. Further studies of the function of Asap in C4da neurons should help elucidate how the diversity of axonal projection patterns and precise neural circuit assembly is achieved during nervous system development.

Materials and Methods

asap-mutant flies were generated by imprecise excision of the NP4638 line. Flp-out and MARCM analyses were performed as previously described, with some modifications (7, 30). Other details of fly genetics, immunostaining, and biochemical analysis are provided in *SI Materials and Methods*. Table S1 gives the fly genotypes used in all experiments.

ACKNOWLEDGMENTS. We thank Y. N. Jan, Y. Hiromi, E. Suzuki, T. Uemura, the Bloomington Stock Center, and the Kyoto Stock Center for fly stocks; Y. Hiromi for cDNAs; J.Z. Parrish and K. Shen for critical reading of the manuscript; the members of the Emoto laboratory, Hiromi laboratory, and Suzuki laboratory for helpful comments and discussions; and Y. Nagashima, C. Ookura, W. Sugano, and A. Kawasaki for expert technical assistance.

1. Brown AG (1981) *Organization in the Spinal Cord* (Springer, New York).
2. Fields HL (1987) *Pain* (McGraw-Hill, New York).
3. Wu Z, et al. (2011) A combinatorial semaphorin code instructs the initial steps of sensory circuit assembly in the *Drosophila* CNS. *Neuron* 70:281–298.
4. Feldheim DA, O'Leary DD (2010) Visual map development: Bidirectional signaling, bifunctional guidance molecules, and competition. *Cold Spring Harb Perspect Biol* 2:a001768.
5. Yoshida Y, Han B, Mendelsohn M, Jessell TM (2006) PlexinA1 signaling directs the segregation of proprioceptive sensory axons in the developing spinal cord. *Neuron* 52:775–788.
6. O'Donnell M, Chance RK, Bashaw GJ (2009) Axon growth and guidance: Receptor regulation and signal transduction. *Annu Rev Neurosci* 32:383–412.
7. Grueber WB, et al. (2007) Projections of *Drosophila* multidendritic neurons in the central nervous system: Links with peripheral dendrite morphology. *Development* 134:55–64.
8. Zlatic M, Li F, Strigini M, Grueber W, Bate M (2009) Positional cues in the *Drosophila* nerve cord: Semaphorins pattern the dorso-ventral axis. *PLoS Biol* 7:e1000135.
9. Grueber WB, Jan LY, Jan YN (2002) Tiling of the *Drosophila* epidermis by multidendritic sensory neurons. *Development* 129:2867–2878.
10. Grueber WB, Ye B, Moore AW, Jan LY, Jan YN (2003) Dendrites of distinct classes of *Drosophila* sensory neurons show different capacities for homotypic repulsion. *Curr Biol* 13:618–626.
11. Sardiello M, Cairo S, Fontanella B, Ballabio A, Meroni G (2008) Genomic analysis of the TRIM family reveals two groups of genes with distinct evolutionary properties. *BMC Evol Biol* 8:225–246.
12. Hattori Y, Sugimura K, Uemura T (2007) Selective expression of Knot/Collier, a transcriptional regulator of the EBF/Olf-1 family, endows the *Drosophila* sensory system with neuronal class-specific elaborated dendritic patterns. *Genes Cells* 12:1011–1022.
13. Jinushi-Nakao S, et al. (2007) Knot/Collier and cut control different aspects of dendrite cytoskeleton and synergize to define final arbor shape. *Neuron* 56:963–978.
14. Lee T, Luo L (1999) Mosaic analysis with a repressible cell marker for studies of gene function in neuronal morphogenesis. *Neuron* 22:451–461.
15. Harris R, Sabatelli LM, Seeger MA (1996) Guidance cues at the *Drosophila* CNS midline: Identification and characterization of two *Drosophila* Netrin/UNC-6 homologs. *Neuron* 17:217–228.
16. Kolodziej PA, et al. (1996) *frazzled* encodes a *Drosophila* member of the DCC immunoglobulin subfamily and is required for CNS and motor axon guidance. *Cell* 87:197–204.
17. Lyulcheva E, et al. (2008) *Drosophila* pico and its mammalian ortholog lamellipodin activate serum response factor and promote cell proliferation. *Dev Cell* 15:680–690.
18. Lai Wing Sun K, Correia JP, Kennedy TE (2011) Netrins: Versatile extracellular cues with diverse functions. *Development* 138:2153–2169.
19. De Vries M, Cooper HM (2008) Emerging roles for neogenin and its ligands in CNS development. *J Neurochem* 106:1483–1492.
20. Lafuente EM, et al. (2004) RIAM, an Ena/VASP and Profilin ligand, interacts with Rap1-GTP and mediates Rap1-induced adhesion. *Dev Cell* 7:585–595.
21. Reymond A, et al. (2001) The Tripartite motif family identifies cell compartments. *EMBO J* 20:2140–2151.
22. Song W, Onishi M, Jan LY, Jan YN (2007) Peripheral multidendritic sensory neurons are necessary for rhythmic locomotion behavior in *Drosophila* larvae. *Proc Natl Acad Sci USA* 104:5199–5204.
23. Hughes CL, Thomas JB (2007) A sensory feedback circuit coordinates muscle activity in *Drosophila*. *Mol Cell Neurosci* 35:383–396.
24. Ainsley JA, et al. (2003) Enhanced locomotion caused by loss of the *Drosophila* DEG/ENaC protein Pickpocket1. *Curr Biol* 13:1557–1563.
25. Adler CE, Fetter RD, Bargmann CI (2006) UNC-6/Netrin induces neuronal asymmetry and defines the site of axon formation. *Nat Neurosci* 9:511–518.
26. Round J, Stein E (2007) Netrin signaling leading to directed growth cone steering. *Curr Opin Neurobiol* 17:15–21.
27. Colón-Ramos DA, Margeta MA, Shen K (2007) Glia promote local synaptogenesis through UNC-6 (netrin) signaling in *C. elegans*. *Science* 318:103–106.
28. Merritt DJ, Whitington PM (1995) Central projections of sensory neurons in the *Drosophila* embryo correlate with sensory modality, soma position, and proneural gene function. *J Neurosci* 15:1755–1767.
29. Kim MD, Jan LY, Jan YN (2006) The bHLH-PAS protein Spineless is necessary for the diversification of dendrite morphology of *Drosophila* dendritic arborization neurons. *Genes Dev* 20:2806–2819.
30. Grueber WB, Jan LY, Jan YN (2003) Different levels of the homeodomain protein cut regulate distinct dendrite branching patterns of *Drosophila* multidendritic neurons. *Cell* 112:805–818.
31. Meroni G, Diez-Roux G (2005) TRIM/RBCC, a novel class of 'single protein RING finger' E3 ubiquitin ligases. *Bioessays* 27:1147–1157.
32. Alexander M, et al. (2010) MADD-2, a homolog of the Opitz syndrome protein MID1, regulates guidance to the midline through UNC-40 in *Caenorhabditis elegans*. *Dev Cell* 18:961–972.
33. Hao JC, et al. (2010) The Tripartite motif protein MADD-2 functions with the receptor UNC-40 (DCC) in Netrin-mediated axon attraction and branching. *Dev Cell* 18:950–960.
34. Song S, et al. (2011) TRIM-9 functions in the UNC-6/UNC-40 pathway to regulate ventral guidance. *J Genet Genomics* 38:1–11.
35. Berti C, Messali S, Ballabio A, Reymond A, Meroni G (2002) TRIM9 is specifically expressed in the embryonic and adult nervous system. *Mech Dev* 113:159–162.